Electronic Supplementary Material (ESI) for RSC Applied Interfaces.

Supporting Information

Zinc Adeninate Metal-Organic Framework-Coated Optical Fibers for Enhanced Luminescence-Based Detection of Rare Earth Elements

Scott E. Crawford,*[a,b] Ward A. Burgess,[a,b] Ki-Joong Kim,[a,b] John P. Baltrus,[a] and Nathan A. Diemler[a,b]

[a]National Energy Technology Laboratory, 626 Cochrans Mill Road, Pittsburgh, Pennsylvania 15236, United States. E-mail: Scott.Crawford@netl.doe.gov

[b]NETL Support Contractor, 626 Cochrans Mill Road, Pittsburgh, Pennsylvania 15236, United States

Table of Contents:

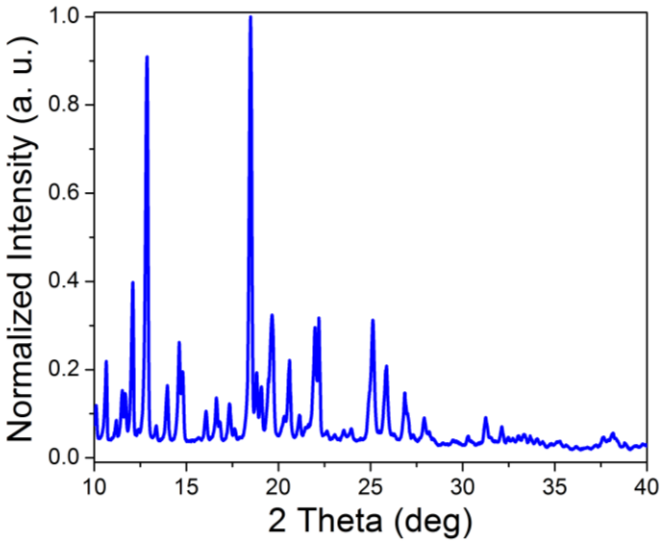

Figure S1. XRD pattern of the BTC-1 MOF. The experimental results are consistent with spectra reported in previous publications for this material.[1,2]

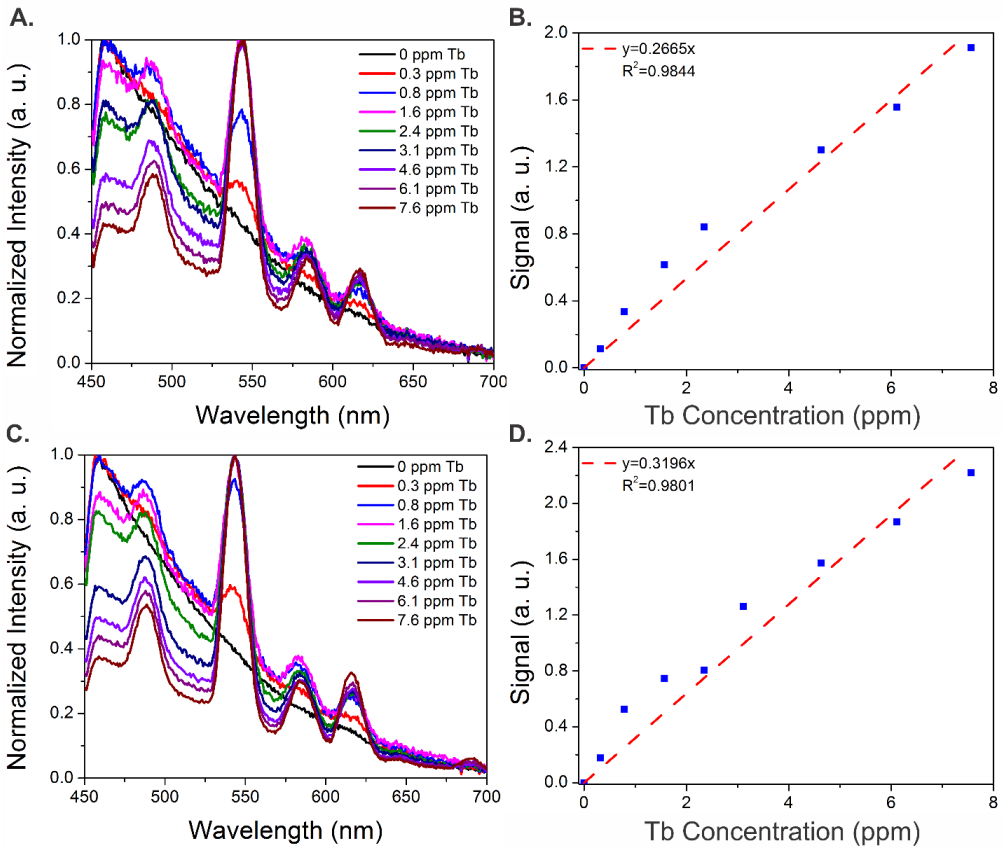

Figure S2. Representative emission spectra of BTC-1 as a function of increasing Tb concentration, normalized to the point of highest intensity, in solution (A) and after drying (C), and the corresponding calibration curve for limit of detection analysis in solution (B) and after drying (D). Signal corresponds to the intensity ratio (I_{543}/I_{453}) at each data point with the (I_{543}/I_{453}) of the MOF alone subtracted.

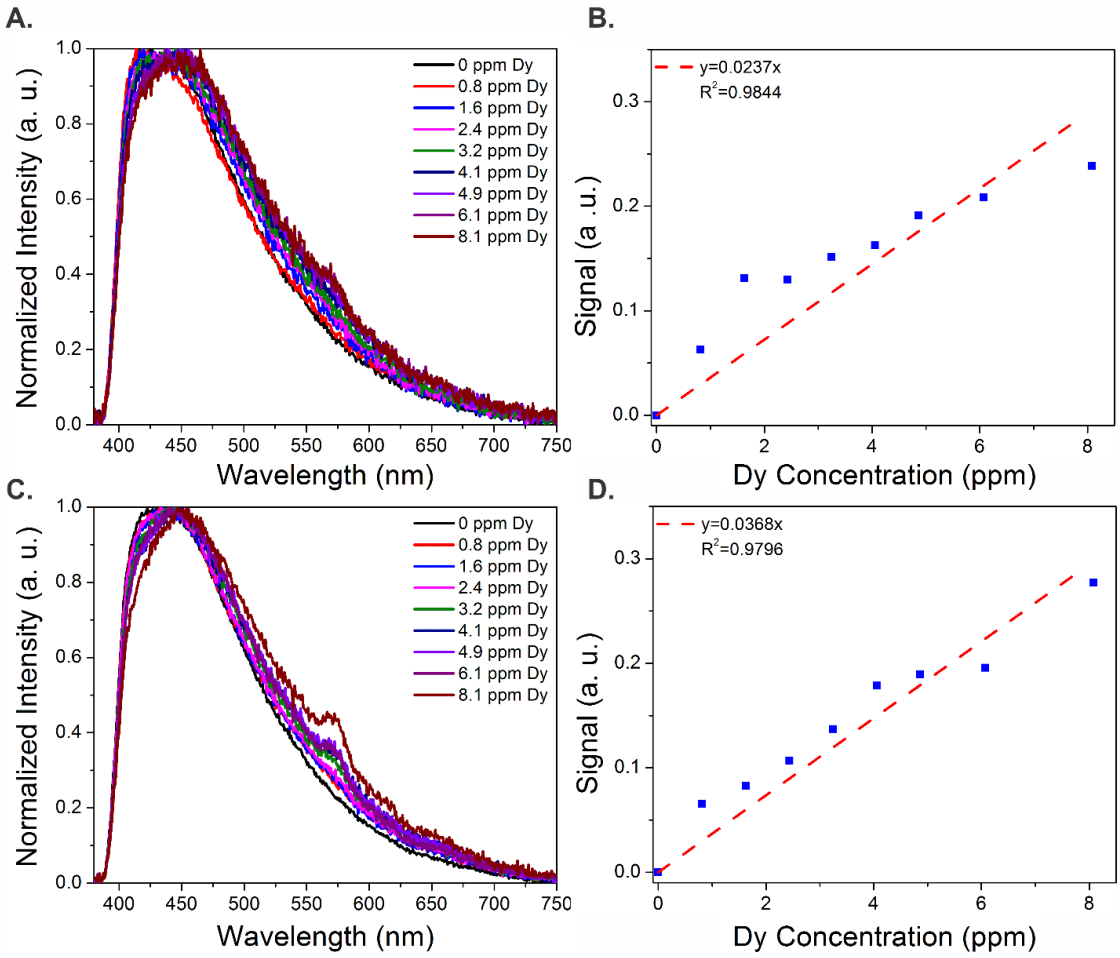

Figure S3. Representative emission spectra of BTC-1 as a function of increasing Dy concentration, normalized to the point of highest intensity, in solution (A) and after drying (C), and the corresponding calibration curve for limit of detection analysis in solution (B) and after drying (D). Signal corresponds to the intensity ratio (I_{573}/I_{453}) at each data point with the (I_{573}/I_{453}) of the MOF alone subtracted.

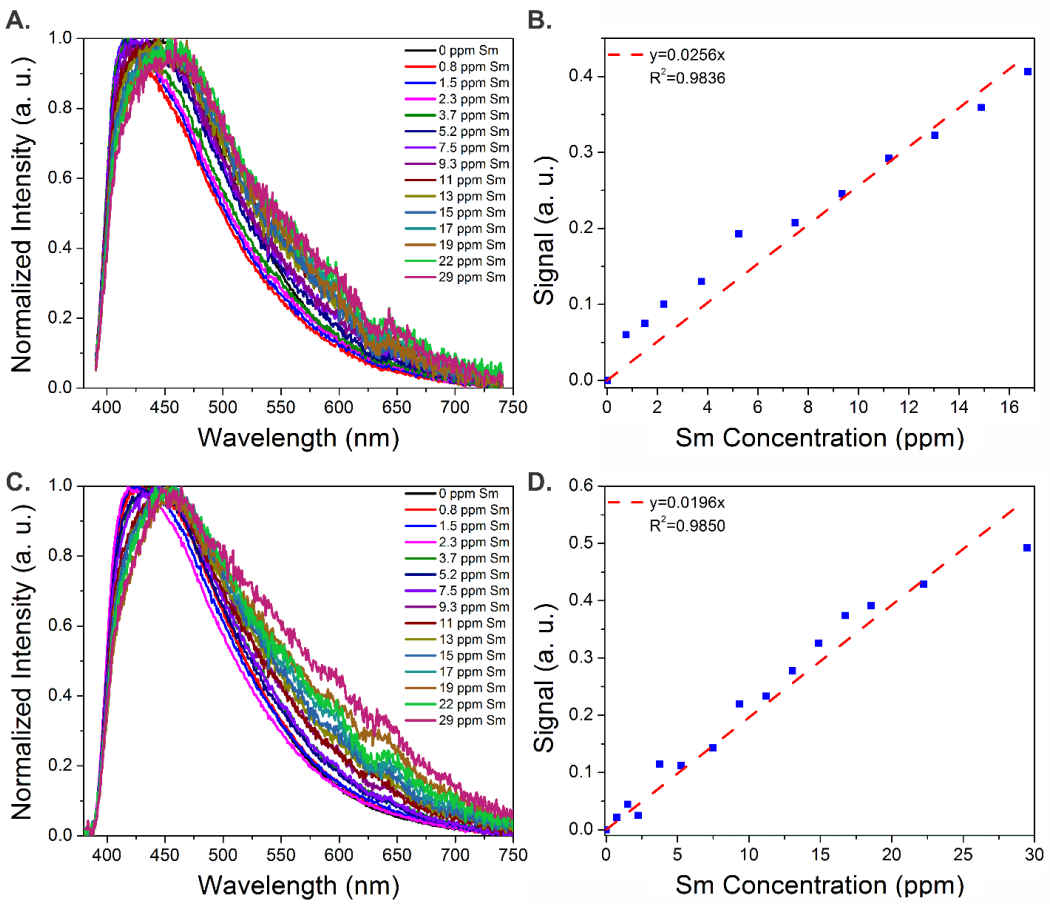

Figure S4. Representative emission spectra of BTC-1 as a function of increasing Sm concentration, normalized to the point of highest intensity, in solution (A) and after drying (C), and the corresponding calibration curve for limit of detection analysis in solution (B) and after drying (D). Signal corresponds to the intensity ratio (I_{597}/I_{453}) at each data point with the (I_{597}/I_{453}) of the MOF alone subtracted.

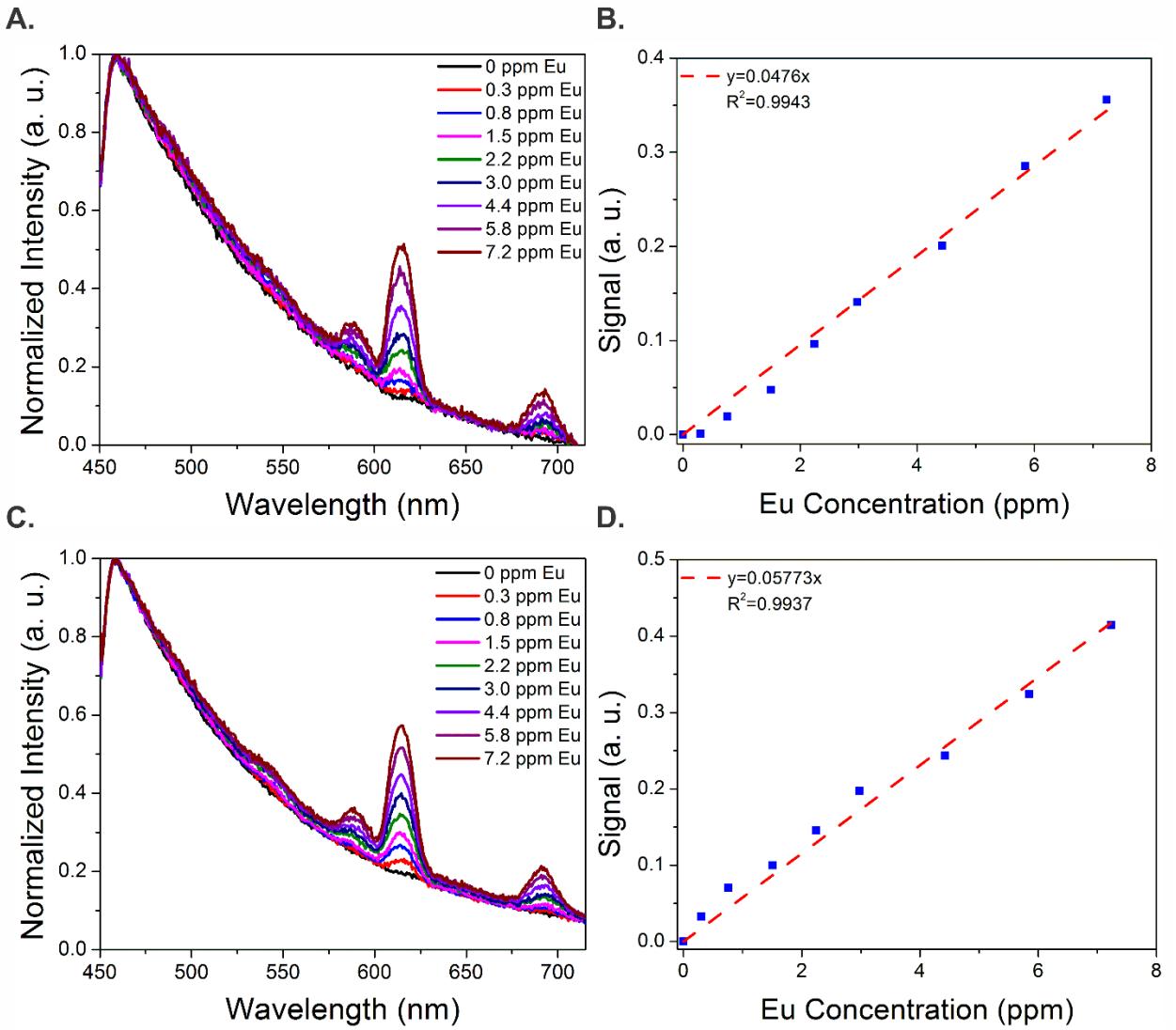

Figure S5. Representative emission spectra of BTC-1 as a function of increasing Eu concentration, normalized to the point of highest intensity, in solution (A) and after drying (C), and the corresponding calibration curve for limit of detection analysis in solution (B) and after drying (D). Signal corresponds to the intensity ratio (I_{613}/I_{453}) at each data point with the (I_{613}/I_{453}) of the MOF alone subtracted.

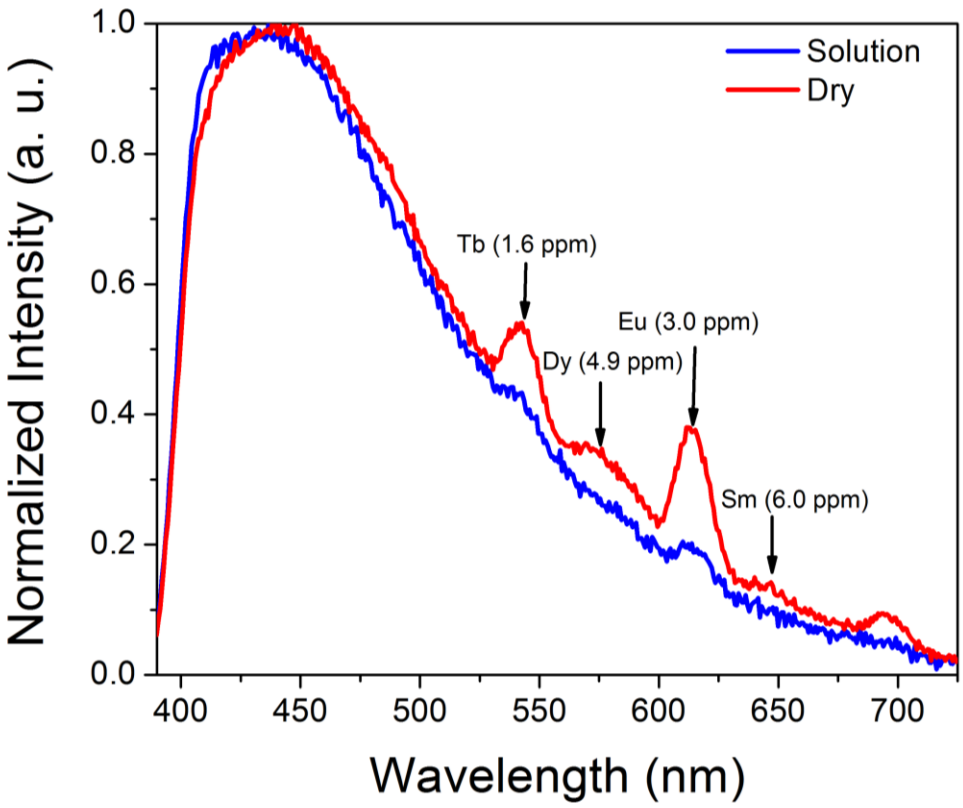

Figure S6. Normalized emission spectra of the BTC-1-coated fiber optic tip exposed to a solution of 1.6 ppm Tb, 4.9 ppm Dy, 3.0 ppm Eu, and 6.0 ppm (Sm) (blue) and after solvent removal (red).

Economic Analysis of Material Cost per Measurement

A rough estimate of the material cost per measurement if the sensing material is discarded after each measurement is included in Table S1. Here, chemical costs are determined using the Sigma Aldrich catalog for each chemical (United States prices, accessed October 17th, 2023) along with the amounts of each reagent used to synthesize BTC-1. The cost per mg or mL of reagent is multiplied to calculate the total reagent cost per synthesis of BTC-1, and we conservatively estimate that each synthetic batch may be used for at least 25 separate measurements. Note that this calculation does not include the miniscule amounts of the sol-gel solution used for coating or the heating costs used to produce the MOFs. The Thorlabs fiber (FG910UEC) costs ~60 to 80 cents per centimeter and would be the most significant material cost if the MOF-coated tip is cleaved after each measurement.

Table S1. Estimated Costs of Reagents Used to Synthesize BTC-1 and Cost Per Measurement

Reagent	Amount Used	Cost per mg or mL ($)	Cost per synthesis ($)
Adenine	33.8 mg	0.0038	0.13
Zinc Acetate Dihydrate	54.9 mg	0.00016	0.009
Trimesic Acid	105 mg	0.00097	0.1
Dimethylformamide	13.5 mL	0.11	1.45
Nitric acid	0.04 mL	0.05	0.002
Cost Per Synthesis			1.69
Cost Per Measurement			**0.068**

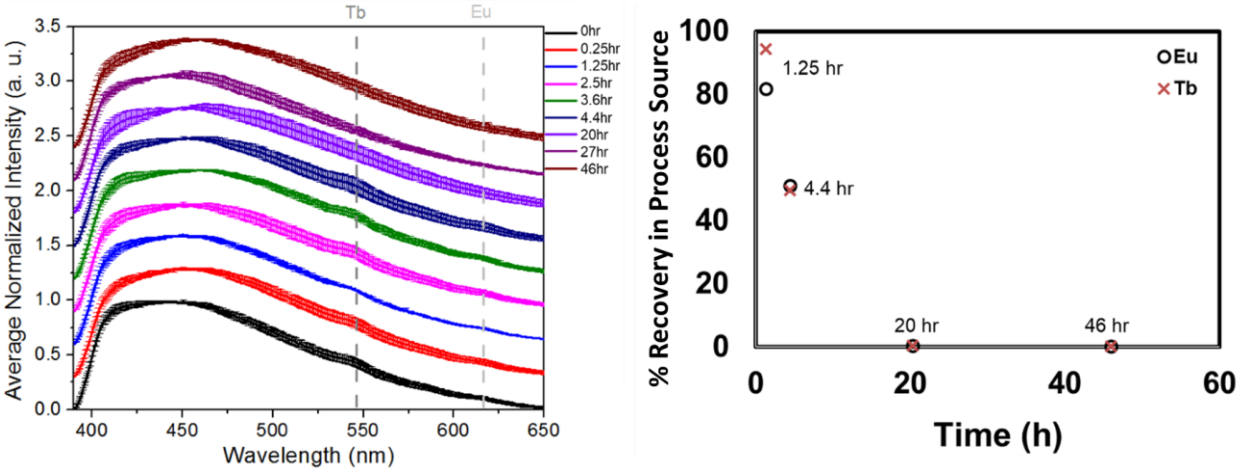

Figure S7. Normalized, stacked emission plots of BTC-1 exposed to the process source solution (left) at different time points (given with units of hours in the legend) after drying during the REE purification process. The line represents the average of three independent trials, with error bars representing the standard error of each measurement. Over time, weak signal from terbium (~545 nm) and europium (~615 nm) decreases, indicating that the concentration of REEs in the process source is decreasing with time. These results are consistent with ICP-MS characterization of terbium and europium in the process source solution over time (right).

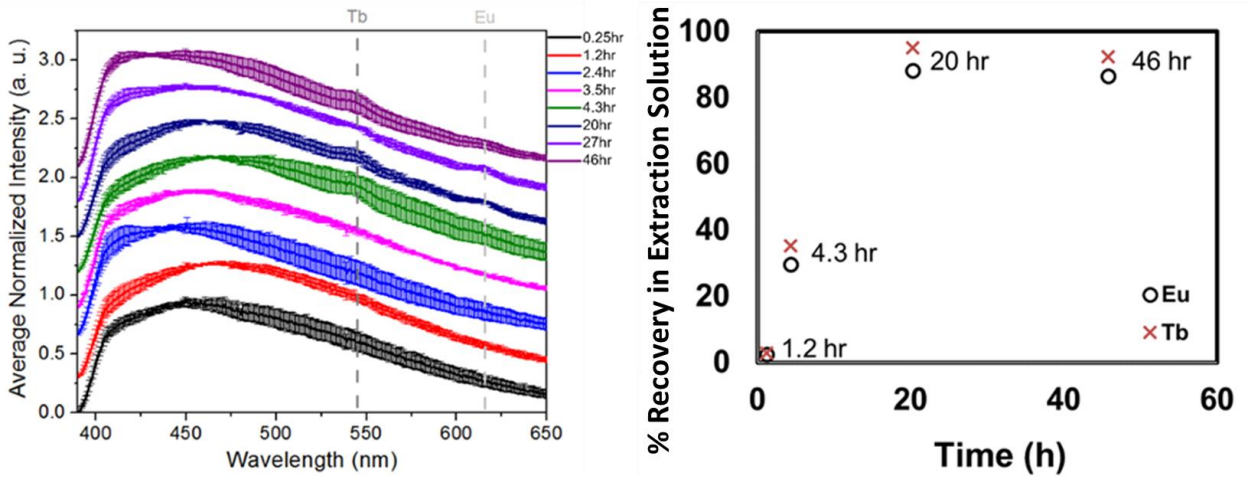

Figure S8. Normalized, stacked emission plots of BTC-1 exposed to the extraction solution (left) at different time points (given with units of hours in the legend) after drying during a REE purification process. The line represents the average of three independent trials, with error bars representing the standard error of each measurement. Signal from terbium (~545 nm) and europium (~615 nm) increases with time in the extraction solution as REEs are transferred, with maximum signal achieved after ~20 hours. These results are consistent with ICP-MS characterization of terbium and europium in the extraction solution over time (right).

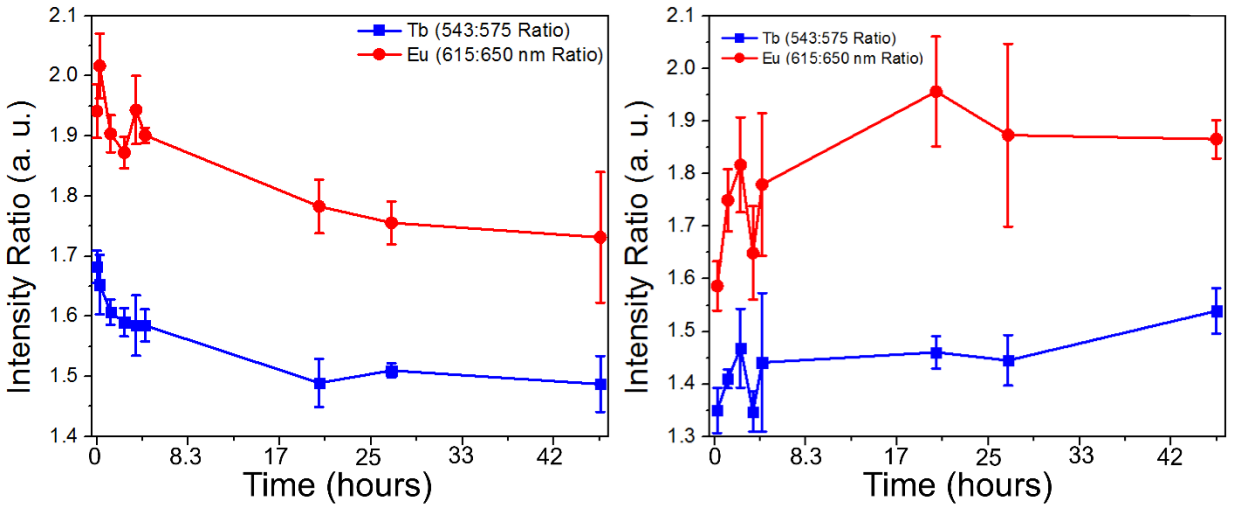

Figure S9. Intensity ratios for Tb (543 nm:575 nm) and Eu (615 nm:650 nm) for the process source solution (left) and the extraction solution (right) taken at different time points using BTC-1 MOF as the sensitizer. Each data point is the average of three trials, with error bars corresponding to the standard error of those measurements. The trends qualitatively match ICP-MS derived values for the same samples as shown in Figures S7 and S8. Ratios here were taken from points associated with the emission maximum from terbium and europium to points at the base of the peak (e.g. 575 nm for Tb and 650 nm for Eu), rather than the MOF peak at ~453 nm, because the MOF peak maximum shifted due to acidic environments.

Table S2. ICP-MS Characterization of process source and extraction solutions at Different Time Points (in ppm)

	Process source						Extraction					
Ion	**0.25hr**	**1.25hr**	**2.5hr**	**4.4hr**	**20hr**	**46hr**	**0.25hr**	**1.2hr**	**2.4hr**	**4.3hr**	**20hr**	**46hr**
Al	3900	4000	4000	4200	4200	4300	16.5	58.0	100	160	320	370
Ca	4000	4000	4100	4400	3800	2800	13	26	43	84	660	1500
K	7300	5300	7400	5600	5600	5800	32	77	-	180	360	420
Y	2.7	2.7	2.5	1.2	0.025	0.024	0.032	0.25	0.47	1.3	4.5	5.1
La	2.9	3.0	2.7	2.4	0.72	0.28	-	-	-	0.18	2.2	2.5
Nd	2.6	2.7	2.7	2.1	0.025	0.021	0.10	0.16	0.23	0.55	2.8	2.8
Eu	**2.4**	**2.4**	**2.3**	**1.5**	**0.012**	**0.010**	**0.013**	**0.078**	**0.19**	**0.89**	**2.6**	**2.5**
Tb	**2.8**	**2.8**	**2.5**	**1.5**	**0.013**	**0.011**	**0.011**	**0.089**	**0.23**	**1.1**	**2.8**	**2.7**

Table S3. ICP-MS Characterization of the Acid Mine Drainage Matrix (pH: 3.3)

Analyte	**Concentration (ppb)**
Li	118
Na	15100
Mg	29330
Al	9840
Si	12560
K	946
Ca	59250
Sc	1.65
Ti	1.00
Cr	2.06
Fe	320
Co	40.8
Ni	108
Cu	12.2

Zn	1290
Sr	810
Y	14.4
Zr	0.153
Cd	1.24
Ba	881
La	6.74
Ce	23.9
Pr	3.72
Nd	17.30
Sm	4.72
Eu	1.23
Gd	4.83
Tb	0.722
Dy	3.38
Ho	0.587
Er	1.51
Tm	0.185
Yb	1.02
Lu	0.139

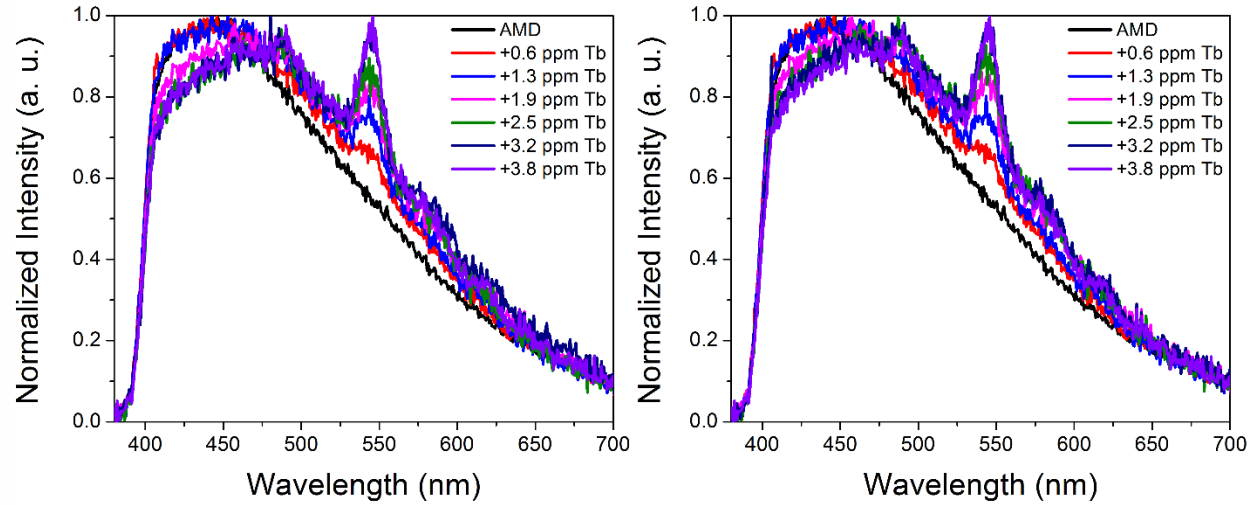

Figure S10. Emission profile of BTC-1 in an acid mine drainage solution (left) exposed to increasing concentrations of terbium, and corresponding emission spectra after drying (right).

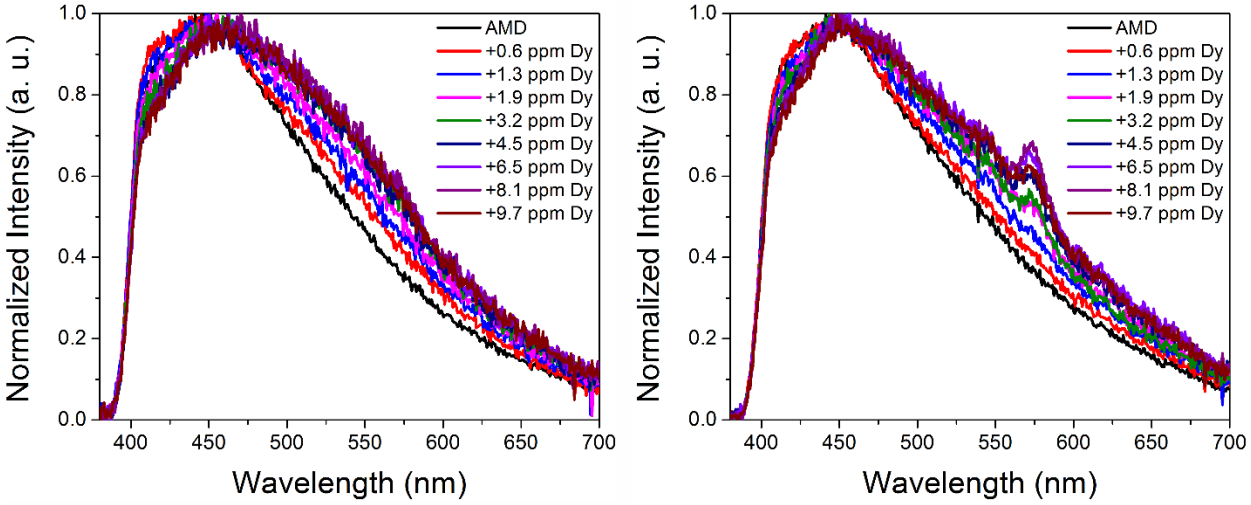

Figure S11. Emission profile of BTC-1 in an acid mine drainage solution (left) exposed to increasing concentrations of dysprosium, and corresponding emission spectra after drying (right).

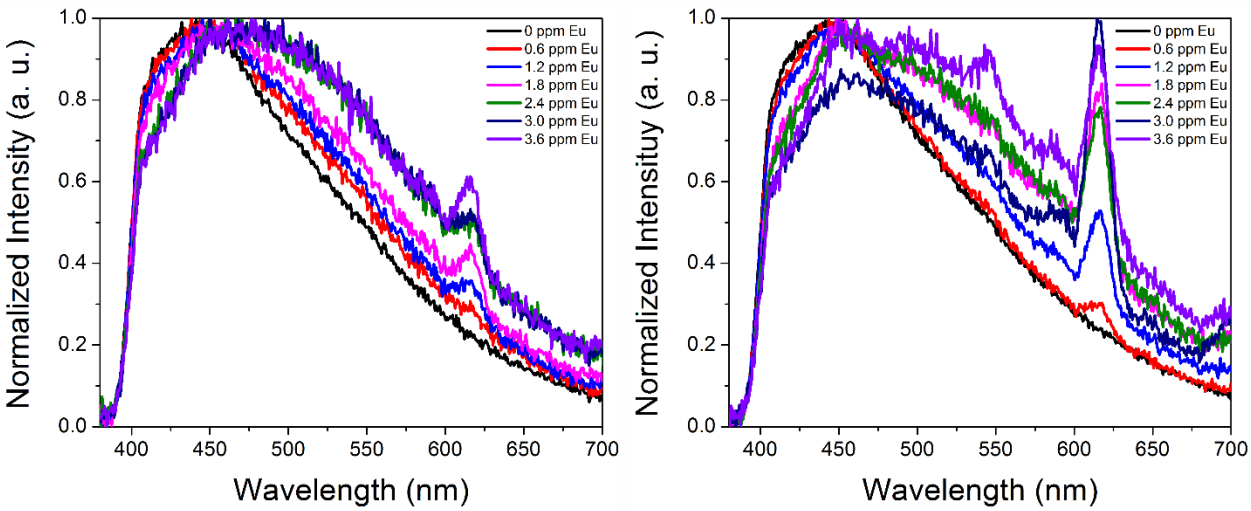

Figure S12. Emission profile of BTC-1 in an acid mine drainage solution (left) exposed to increasing concentrations of europium, and corresponding emission spectra after drying (right).

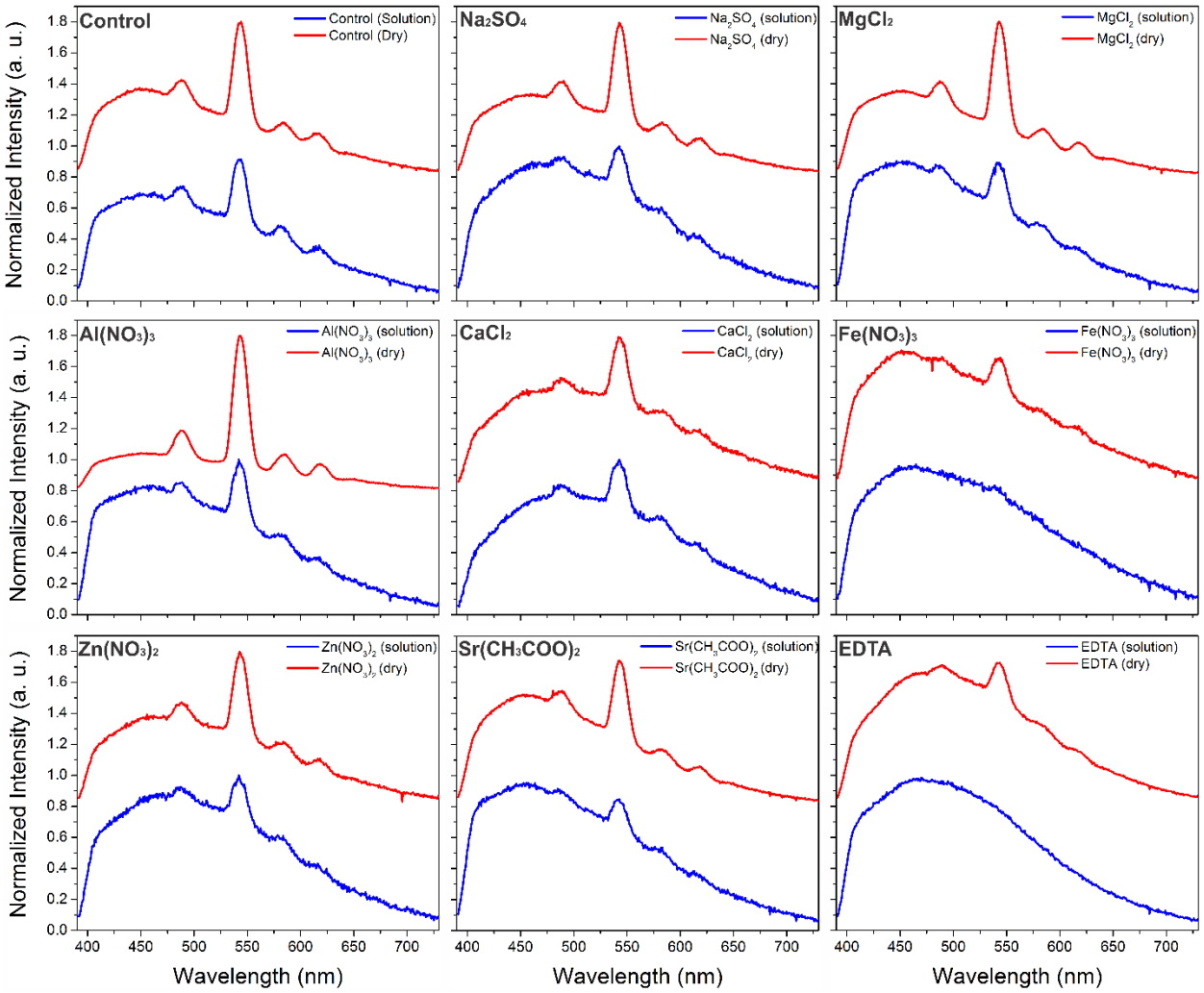

Figure S13. Representative emission spectra of 25 µm $Tb(NO_3)_3$ and 2500 µm of various metal salts in solution and after drying, as well as a sample containing 25 µm $Tb(NO_3)_3$ and 25 µm of EDTA. A control trial containing only 25 µm $Tb(NO_3)_3$ in water is also shown for comparison. Spectra are normalized and offset by 0.8 on the y-axis for clarity.

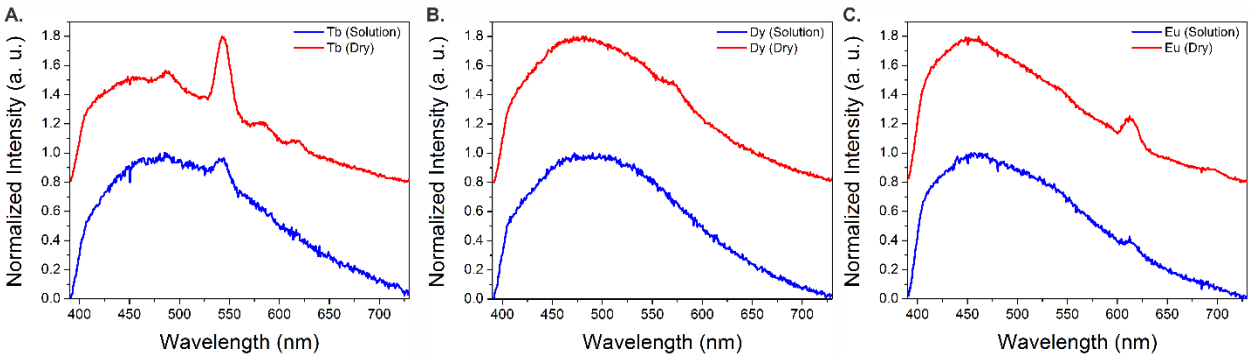

Figure S14. Representative emission spectra of 25 µm of (A) $Tb(NO_3)_3$, (B) $Dy(NO_3)_3$, and (C) $Eu(NO_3)_3$ with 2500 µm each of $Fe(NO_3)_3$, $Al(NO_3)_3$, $Zn(NO_3)_2$, $Sr(CH_3COO)_2$, $CaCl_2$, $MgCl_2$, and Na_2SO_4. Spectra are normalized and offset by 0.8 on the y-axis for clarity.

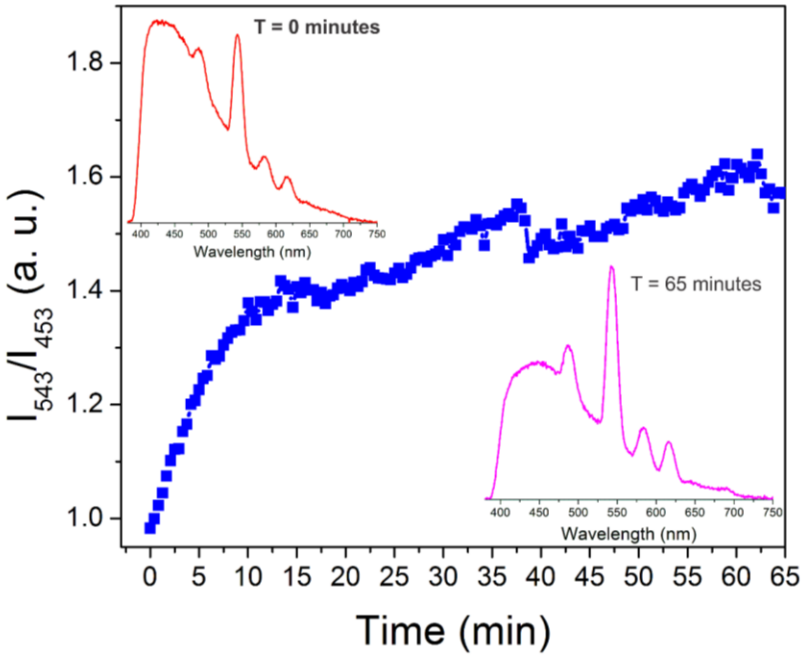

Figure S15. Ratio of the Tb emission peak at 543 nm vs the MOF emission peak at 453 nm (I_{543}/I_{453}) as a function of time while stirring at 1150 rpm in a 4 ppm Tb solution. The Tb emisison signal increases over time with stirring (Insets: emission spectra taken at the beginning and end of the experiment)

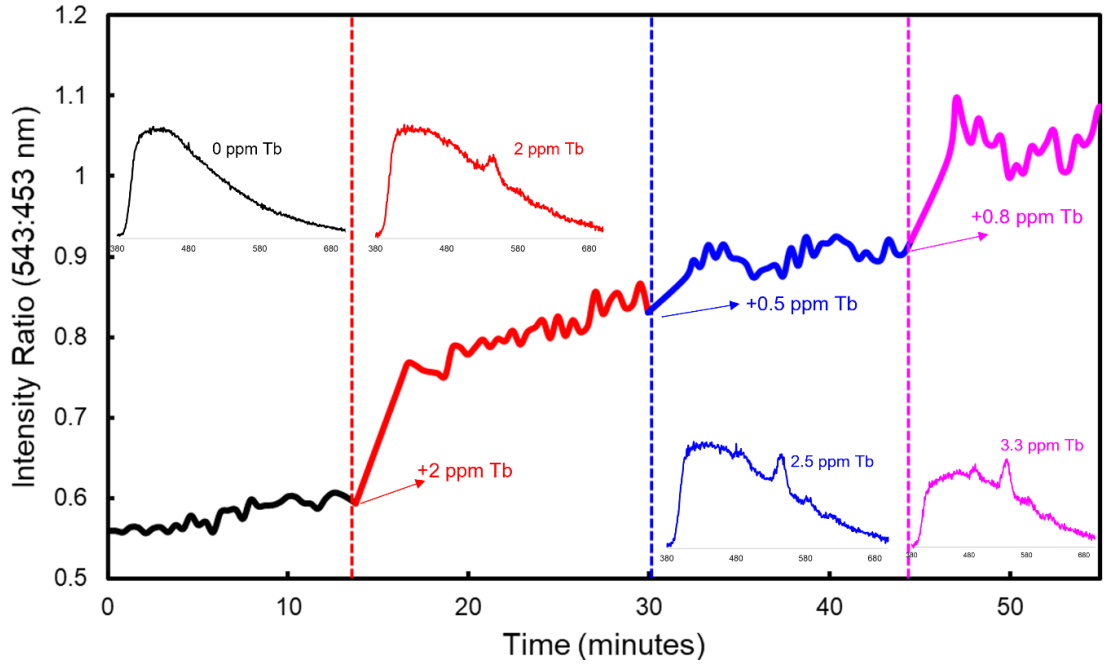

Figure S16. Ratio of the Tb emission peak at 543 nm vs the MOF emission peak at 453 nm (I_{543}/I_{453}) monitored as a function of time, where spikes of Tb of different concentrations were added at various time points for real-time monitoring of Tb concentration. Insets show individual emission spectra recorded after each Tb addition.

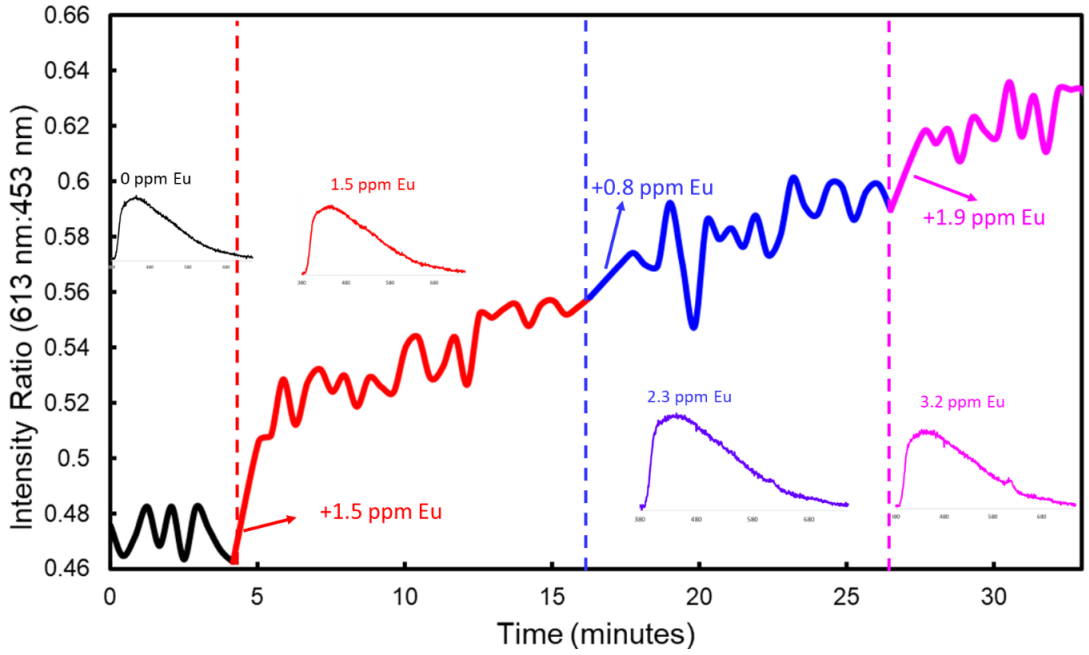

Figure S17. Ratio of the Eu emission peak at 613 nm vs the MOF emission peak at 453 nm (I_{613}/I_{453}) monitored as a function of time, where spikes of Eu of different concentrations were added at various time points for real-time monitoring of Eu concentration. Insets show individual emission spectra recorded after each Eu addition.

References

1. S. E. Crawford, J. E. Ellis, P. R. Ohodnicki and J. P. Baltrus, *ACS Appl. Mater. Interfaces,* 2021, **13**, 7268-7277.
2. J. An, S. J. Geib, M.-G. Kim, S. Y. Choi and W. T. Lim, *J. Porous Mater.*, 2015, **22**, 867-875.